EPJ manuscript No.
(will be inserted by the editor)

Spectroscopy of orbital ordering in $La_{0.5}Sr_{1.5}MnO_4$: A many-body cluster calculation

Alessandro Mirone[1], S.S. Dhesi[2], G. van der Laan[3]
[1]European Synchrotron Radiation Facility, BP 220, F-38043 Grenoble Cedex, France
[2] Diamond Light Source,Chilton, Didcot, OX11 0DE, United Kingdom
[3]CCLRC Daresbury Laboratory, Warrington WA4 4AD, United Kingdom

Received: date / Revised version: date

Abstract. We have studied the orbital ordering (OO) in $La_{0.5}Sr_{1.5}MnO_4$ and its soft x-ray resonant diffraction spectroscopic signature at the Mn $L_{2,3}$ edges. We have modelled the system in second quantization as a small planar cluster consisting of a central Mn atom, with the first neighbouring shells of oxygen and Mn atoms. For the effective Hamiltonian we consider Slater-Koster parameters, charge transfer and electron correlation energies obtained from previous measurements on manganites. We calculate the OO as a function of oxygen distortion and spin correlation used as adjustable parameters. Their contribution as a function of temperature is clearly distinguished with a good spectroscopic agreement.

PACS. 61.10.-i X-ray diffraction and scattering – 71.30.+h Metal-insulator transitions and other electronic transitions – 71.10.-w Theories and models of many-electron systems – 78.20.Bh Theory, models, and numerical simulation

1 Introduction

Recent soft x-ray resonant diffraction measurements on half-doped manganite $La_{0.5}Sr_{1.5}MnO_4$ have been interpreted in terms of orbital ordering (OO) [1,2,3]. There is a strong interest in understanding how OO settles in this system as a result of the interplay between charge, orbital and spin degrees of freedom. In fact, this interplay can be found in many other different phenomena, such as high-temperature superconductivity, colossal magnetoresistance and magnetostructural transitions [4].

The MnO_2 plane with its superstructure for half doping at low temperature is shown in Figure 1 [5,6,7,8,9,10]. The two charge-separated Mn sites, which we shall denote by Mn^{3+} and Mn^{4+} (although the charge separation is fractional) display a checker board alternation. One can see ferromagnetic zig-zag chains, where the Mn^{4+} sites form the corners and the Mn^{3+} sites are in the middle of the straight segments. Adjacent zig-zag chains are antiferromagnetically aligned with respect to each other. There is a distortion of the oxygen atoms consisting of an elongation of the Mn^{3+}-O bonds along the zig-zag segments. Figure 1 shows the occupied Mn^{3+} e_g orbital under the hypothesis of $3z^2{-}r^2$/ $3x^2{-}r^2$ ordering, which is a possible simplified way of looking at the electronic structure, although so far there is not yet a consensus regarding the correct ordering. More importantly, there is no consensus yet regarding the way the OO and spin-ordering settle in the system as a function of temperature.

Based on recent soft x-ray resonant diffraction experiments we will try to answer these still open questions with a theoretical analysis of the spectra. The soft x-ray resonant diffraction experiments that we consider have been done on $La_{0.5}Sr_{1.5}MnO_4$ at the Mn $L_{2,3}$ edges where the scattering factors exhibit huge variations with a strong dependence on the precise $3d$ orbital occupation and ordering.

Considering the stoichiometry in $La_{0.5}Sr_{1.5}MnO_4$, the average occupation of the Mn $3d$ shell can be estimated at about 3.5 electrons. The soft x-ray diffraction spectra show a strong multiplet structure due to transitions $3d^n \leftrightarrow 2p^5 3d^{n+1}$ [11] which are complicating the analysis. Previous studies [1,2,3] simplified the analysis of the multiplet structure by considering integer charge ordering (CO) with a $3d$ occupation of 4 electrons on the active sites (active in the OO diffraction process). The scattering factors of the active site (Mn^{3+}) were then calculated in the crystal-field approximation. Although such calculations were able to produce some reminiscence of the observed spectra, the agreement was not good enough to clearly discriminate between the different hypotheses concerning the occupied orbitals. Moreover, these calculations were based on a local mean-field approximation and were inherently unable to treat the effects of spin correlation between the different Mn sites. The approximation of integer occupation is contrasting with band calculations results, which estimate the charge separation between Mn sites to be about 0.3 (Ref. [12]) instead of one electron.

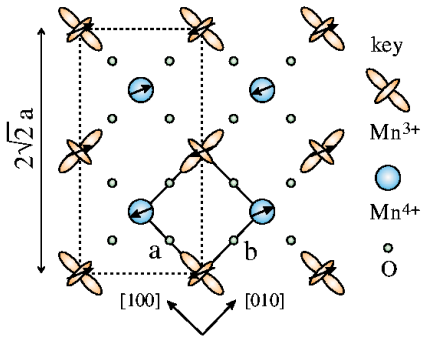

Fig. 1. The MnO_2 plane and its super structure in the case of half doping at low temperature.

In this work we will go beyond the limits of previous analyses, by building a cluster around the active Mn site. We consider a model where the degenerate $3d$ shell of the active site is coupled to the neighbouring oxygen orbitals by hopping terms. On their turn, the oxygen orbitals are coupled to the $3d$ orbitals of the inactive Mn^{4+} sites (these for symmetry reasons inactive sites do not contribute to the OO diffraction). For the inactive Mn sites we consider only one e_g orbital. For this orbital we add a spin-dependent energy term to simulate the spin magnetisation. In this model we can play with two main ingredients, i.e., the distortion of the oxygen positions (Jahn-Teller distortion) which rescales the hopping, and the spin magnetisation of the inactive sites.

In Sec. 2 we define the Hamiltonian and in Sec. 3 we fix the parameters. In Sec. 4 we compare the experimental spectra to the calculated spectra obtained by choosing an optimal distortion. The study of the dependence of the calculated spectra on distortion and spin magnetisation is summarized in Sec. 5.

2 Model Hamiltonian

We consider a model where the degenerate $3d$ electrons of the active site are coupled to the neighbouring oxygen orbitals by a hopping term modulated by Slater-Koster parameters. The oxygen orbitals are on their turn coupled to the $3d$ orbitals of the inactive Mn^{4+} sites. The Hamiltonian of the total system is

$$H = H_a + T_1 + T_2 + H_1 + H_2\,, \tag{1}$$

where H_a is the atomic Hamiltonian for the active Mn site and H_1 and H_2 are the Hamiltonians for the first-neighbour oxygen atoms and the neighbouring inactive Mn^{4+} sites, respectively, in the absence of hopping. The T_1 and T_2 are the hopping terms for the Mn^{3+}-O and O-Mn^{4+} bonds, respectively.

$$T_1 = \sqrt{2}\,t \sum_\sigma \left(g\, o^\dagger_{x,\sigma} d_{x^2,\sigma} + o^\dagger_{z,\sigma} d_{z^2,\sigma} + o^\dagger_{y,\sigma} d_{y^2,\sigma}\right) + \text{c.c.}, \tag{2}$$

where the z and x axes lie in the MnO_2 plane, t is the Slater-Koster V_σ parameter, g is the reduction factor of the hopping along x (which is taken parallel to the zig-zag segment). The d and o are the second-quantization operators for Mn $3d$ and O $2p$ electrons, respectively. Neglecting the smaller V_π parameter, we consider only three oxygen orbitals (six including spin) and $o_{x,y,z}$ represents the orbitals in the x,y,z directions. Only one oxygen per direction is considered and a factor $\sqrt{2}$ is included in T_1, so that the o's represent symmetrized orbitals. The d_{x^2}, d_{y^2} and d_{z^2} are linear combinations of e_g operators pointing along the three cartesian directions (e.g., $d_{x^2} = \sqrt{3}/2\, d_{x^2-y^2} + 1/2\, d_{z^2}$). The o_z and o_x degrees of freedom are on their turn coupled to two Mn^{4+} sites by a hopping term

$$T_2 = t \sum_\sigma \left(o^\dagger_{x,\sigma} X_\sigma + o^\dagger_{z,\sigma} Z_\sigma\right) + \text{c.c.}, \tag{3}$$

where X (Z) represents an e_g orbital at the Mn^{4+} site along the X (Z) direction.

The Hamiltonian H_1 for the isolated oxygen atoms is

$$H_1 = \sum_i [\epsilon_p \sum_\sigma o^\dagger_{i,\sigma} o_{i,\sigma} + U_{pp}(1 - o^\dagger_{i\uparrow} o_{i\uparrow})(1 - o^\dagger_{i\downarrow} o_{i\downarrow})], \tag{4}$$

with $i \in \{x, y, z\}$. The Hamiltonian H_2 is

$$H_2 = \sum_\sigma [\epsilon_d + h(\frac{1}{2} + \sigma_z)] X^\dagger_\sigma X_\sigma + \sum_\sigma [\epsilon_d + h(\frac{1}{2} - \sigma_z)] Z^\dagger_\sigma Z_\sigma, \tag{5}$$

where h is the exchange energy term that takes into account the opposite magnetisation of the two Mn^{4+} sites. The Hubbard correlation term is absent in H_2, but in the calculation we limit the Hilbert space by disregarding states with doubly occupied X or Z orbitals.

3 Choice of parameters

The parameters for the atomic Hamiltonian H_a, which are the spin-orbit interactions and Slater integrals – except for the monopole terms which are strongly screened – have been obtained using Cowan's Hartree-Fock code [13] averaging the values for the Mn^{3+} and Mn^{4+} configurations. The atomic parameters are listed in Table 1. We apply rescaling factors of 0.75 and 0.8 to the dd and pd Slater integrals, respectively, as is common practise to obtain effective Slater integrals for correlated transition metal systems [11]. For F^0_{dd} we start from the estimated U_{dd} of about 5 eV from previous studies [12] based on spectroscopical data. Considering a starting configuration $t^3_{2g\downarrow} e^1_{g\downarrow}$ and adding two extra electrons we obtain $t^3_{2g\downarrow} e^2_{g\downarrow} t^1_{2g\uparrow}$. Therefore the experimental U_{dd} is the interaction between a $t_{2g\uparrow}$ and an $e_{g\downarrow}$ electron,

$$U_{dd} = F^0_{dd} - 4/49\, F^2_{dd} - 2/147\, F^4_{dd}, \tag{6}$$

from which F^0_{dd} is deduced.

The hopping t is estimated as 1.8 eV and U_{pp} as 5 eV. The bare energy ϵ_p of the oxygen orbitals is deduced

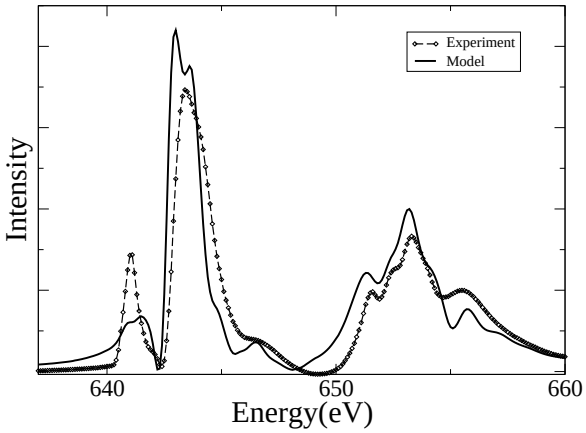

Fig. 2. Experimental diffraction spectrum (dashes with diamonds) and calculation (solid line) for an optimal distortion and correlation.

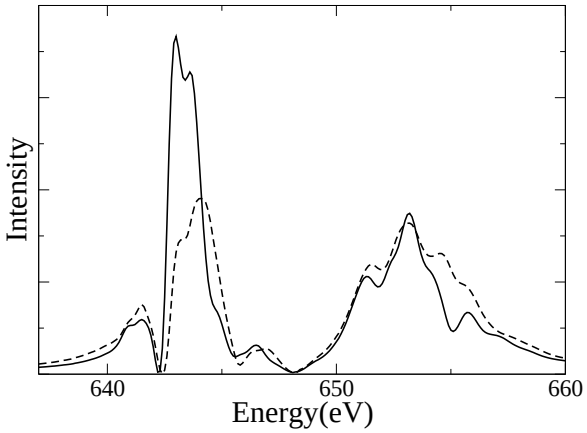

Fig. 3. Calculated diffraction spectra for different values of the distortion and magnetic correlation parameter. Solid line is for $g = 0.7$; $h = 2.5$. Dashed line is for $g = 0.85$; $h = 1.25$.

from the charge-transfer energy $\Delta = 4$ eV. This experimental parameter is defined as the energy to transfer an oxygen electron onto a bare Mn atom (in the absence of hybridization). Therefore,

$$\epsilon_p = -\Delta + n_d F^0_{dd} + 6F^0_{pd} - 14/49\, F^2_{dd} - 14/49\, F^4_{dd} \\ -2/5\, G^1_{pd} - 9/35\, G^3_{pd} + (2 - n_p)U_{pp} + \delta_{\rm hyb}, \quad (7)$$

where n_d and n_p are the average occupation numbers of the Mn $3d$ and O $2p$ shell, respectively, in the ground state of the model Hamiltonian and $\delta_{\rm hyb}$ is the residual energy shift of the oxygen orbitals when we consider hybridization with inactive sites only. The value that we find is $\epsilon_p = 54.9$ eV. Of course, such a large energy value is not referenced to the vacuum level but to a bare $3d$ orbital with zero occupation. The spin-magnetisation parameter h for the Mn^{4+} sites is 2.5 eV in the case of full spin ordering. The energy of the bare orbitals X and Z is

$$\epsilon_d = \epsilon_p + \Delta + \delta_d\,, \quad (8)$$

where δ_d is a free parameter that is allowed to take values in the order of 1 eV, which accounts for different effects, such as the charge splitting between the sites and an additional effective ligand field that compensates for the incomplete inclusion of hybridization for the X and Z orbitals in the model. The spin quantization axis $\acute{z}$ in Eq. 5, which fixes the orientation of the magnetisation for the Mn^{4+} sites, lies in the (001) plane and we have tested several different orientations.

4 Results

Figure 2 shows the calculated spectrum for a hybridization reduction factor $g = 0.7$ and a Mn^{4+} energy term $\delta_d = 0.8$ eV. In the calculation the Hilbert space of the ground-state configuration and the excited-state configuration (with a $2p$ hole and an extra electron in the valence band) have been fully expanded with the constraint to have between 8 and 12 electrons on the Mn^{4+} sites and zero or one electron in each of the X, Z orbitals. The scattering factors are calculated in the dipole approximation and using a Lorentzian line width broadening of 0.45 (0.55) eV for the L_3 (L_2) edge. The magnetisation is taken along the [110] direction which gives the best fit. The reflectivity is calculated as the squared OO scattering factor divided by the absorption of the sample [1]. The absorption is calculated as a stoichiometric average of the $La_{0.5}Sr_{1.5}MnO_4$ elemental absorption. The absorption for Mn is obtained using the experimental absorption measured for $La_{0.5}Sr_{1.5}MnO_4$ [1] at the $L_{2,3}$ absorption edges and joining it with the tabulated values. The experimental spectrum has been measured at 134 K [1].

Our calculation reproduces all the spectral features, the only problem is that the right-hand shoulder of the lowest energy peak has too much intensity and appears as a separate peak. It is interesting to look at the behavior of the system as a function of the oxygen displacement. Going from zero distortion ($g \simeq 1$) to strong distortion ($g < 0.5$) we have observed that the L_3 peak is already dominant at very low distortion ($g \simeq 1$), while at lower g values it loses intensity compared to the L_2 peak. This result is very different from all previous analyses based on simple ligand-field models [14], which predict a direct relation between the L_3 main peak intensity and the Jahn-Teller distortion. We think that the ligand-field model may fail in this case because the resonant diffraction is sensitive to the scattering factor differences for different polarisations and these differences depend not only on one-particle energy shifts but also (thinking in terms of one-particle Green functions) on the spectral weight transfer

Configuration	F^2_{dd}	F^4_{dd}	ζ_{3d}	F^2_{pd}	G^1_{pd}	G^3_{pd}	ζ_{2p}	F^0_{dd}	F^0_{pd}
Ground state	8.94	5.62	0.051	5.86	4.38	2.5	–	5.7	$1.1F^0_{dd}$
Excited state	9.53	5.98	0.063	5.86	4.38	2.5	6.85	5.7	$1.1F^0_{dd}$

Table 1. Calculated atomic Hartree-Fock values [13] for the configuration averaged Slater integrals and spin-orbit interactions (in eV).

due to hybridisation, which ligand-field model neglects. We think that, as a consequence, ligand-field model calculations tend to give stronger splitting of $3d$ orbitals to compensate for the missing spectral weight effect, in particular Stojic et. al [10] find a 1.35eV splitting for the t_{2g} band. Such a value seems unusual to us.

We obtained the optimal fit for $g = 0.7$. For g values between 1 and 0.6 the magnetisation of the Mn^{3+} site is parallel to that of the Mn^{4+} site which lies along the X direction. For g values below 0.6 the magnetisation is reversed. What happens is that the e_g orbital, laying along the $3x^2-r^2$, aligns its spin parallel to that of the Mn^{3+} atom which is found in the Z direction because for too small g the effective hopping on the X orbital becomes weaker than on the Z orbital. However this phenomenon could be an artefact of our model. In fact, the model neglects the t_{2g} hybridization which always gives an antiferromagnetic coupling with the Z orbital. In any case beyond this, possibly artificial, magnetisation-reversal threshold the L_3 main peak is strongly enhanced compared to the L_2 and it shifts to lower energy by about 1.5 eV. This behavior resembles what happens in the case of the $Pr_{0.6}Ca_{0.4}MnO_3$ system below T_N [15]. It is interesting to test with the model to see what happens when the spin correlation is reduced. Our model, in particular the H_2 term in Eq. 5, considers a well established spin order and is simplified by using symmetrized orbitals. A way to mimic the reduction of the spin correlation, without losing the simplicity of the model, is reducing the value of h in Eq. 5. We show in Figure 3, with the solid line, the diffraction spectra for reduced values of the distortion ($g = 0.85$) and spin correlation ($h = 1.25$ eV). The solid line is the optimal fit to the experimental data (from Figure 2). The change in peak heights reproduces the experimental behavior between T_C and T_N [1], i.e., the main L_3 peak loses intensity and the right and left shoulders of the L_2 gain in intensity.

Analysing the one-particle Green function for the ground state we find that in our model the e_g electron spends only 15% of its time on the Mn^{4+} site. This is a very pronounced charge separation. We also find that the occupied e_g orbital at the Mn^{3+} site has $3x^2-r^2$ symmetry. This result contradicts the interpretation of the experimental x-ray linear dichroism at the Mn $L_{2,3}$ edges by Huang *et al.* [16]. They have observed a stronger absorption for in-plane linear polarisation than for out-of-plane polarisation, from which they deduce that the occupied e_g orbital at the active sites has $x^2 - y^2$ symmetry.

5 Conclusion

We have analysed the experimental soft x-ray resonant diffraction of the orbital ordering in the half-doped manganite $La_{0.5}Sr_{1.5}MnO_4$ using a many-body cluster calculation. The dependence on the order parameters of the peak intensities calculated by our model is very different – if not completely opposite – to those found using simpler ligand-field models. In our model a central Mn^{3+} site hybridizes with the first shell of neighbouring oxygen atoms. On their turn the oxygen atoms are hybridized with neighbouring Mn^{4+} atoms in the MnO_2 plane. The experimental spectrum at 134 K has been reproduced with good agreement, using a slight distortion of the planar oxygens and by supposing a strong local magnetic correlation between Mn sites. The temperature dependence of the spectra between T_C and T_N has been reproduced by reducing simultaneously the oxygen distortion and the spin correlation. It is not possible to reproduce the temperature dependence of the spectra between T_C and T_N by simply reducing the distortion. This shows that spin correlation is an important ingredient between T_C and T_N and increases with the lattice distortion. We also found a pronounced charge separation between the two sites and an in-plane orbital polarisation. The latter does not yet allow us to explain the the results of some recent x-ray linear dichroism observations.

We thank the ESRF computing service for computation of the spectra, in particular Wolf Dieter Klotz and Gaby Forstner for taking care of computer clusters and grid computing.

References

1. S.S. Dhesi, A. Mirone, C. Nadai, P. Ohresser, P. Bencok, N.B. Brookes, P. Reutler, A. Revcolevschi, A. Tagliaferri, O. Toulemonde, G. van der Laan, Phys. Rev. Lett. **92**, 056403 (2004)
2. S.B. Wilkins, N. Stojic, T.A.W. Beale, N. Binggeli, C.W.M. Castleton, P. Bencok, D. Prabhakaran, A. T. Boothroyd, P.D. Hatton, M. Altarelli, Phys. Rev. B **71**, 245102 (2005)
3. U. Staub, V. Scagnoli, A.M. Mulders, K. Katsumata, Z. Honda, H. Grimmer, M. Horisberger, J.-M. Tonnerre, Phys. Rev. B **71**, 214421 (2005)
4. I.S. Osborne, Science **288**, 451 (2000)
5. P.G. Radaelli, D.E. Cox, M. Marezio, S.-W. Cheong, Phys. Rev. B **55**, 3015 (1997)
6. T. Mutou, H. Kontani, Phys. Rev. Lett. **83**, 3685 (1999)
7. D. Khomskii, J. van den Brink, Phys. Rev. Lett. **85**, 3329 (2000)
8. T. Hotta, E. Dagotto, H. Koizumi, Y. Takada, Phys. Rev. Lett. **86**, 2478 (2001)

9. A. Daoud-Aladine, J. Rodriguez-Carvajal, L. Pinsard-Gaudart, M.T. Fernández-Diaz, A. Revcolevschi Phys. Rev. Lett. **89**, 097205 (2002)
10. N. Stojic, N. Binggeli, M. Altarelli, Phys. Rev. B **72**, 104108 (2005)
11. G. van der Laan, B.T. Thole, Phys. Rev. B **43** 13401 (1991)
12. T. Mizokawa, A. Fujimori Phys. Rev. B **56** R493 (1997)
13. R.D. Cowan, *The Theory of Atomic Structure and Spectra* (University of California Press, Berkeley, 1981)
14. C.W.M. Castleton, M. Altarelli, Phys. Rev. B **62**, 1033 (2000)
15. K.T. Thomas, J.P. Hill, S. Grenier, Y.-J. Kim, P. Abbamonte, L. Venema, A. Rusydi, Y. Tomioka, Y. Tokura, D.F. McMorrow, G. Sawatazky, M. van Veenendaal, Phys. Rev. Lett. **92**, 237204 (2004)
16. D.J. Huang, W.B. Wu, G.Y. Guo, H.-J. Lin, T.Y. Hou, C.F. Chang, C.T. Chen, A. Fujimori, T. Kimura, H.B. Huang, A. Tanaka, T. Jo, Phys. Rev. Lett. **92**, 087202 (2004)